Front. Optoelectron. China 2008, 1(3–4): 345–351
DOI 10.1007/s12200-008-0044-y

RESEARCH ARTICLE

Fringe-contoured-window sine/cosine filter for saw-tooth phase maps in ESPI

Sihua FU (✉)[1], Xuejun LONG[1], Hui LIN[2], Qifeng YU[1]

1 College of Opto-electronic Science and Engineering, National University of Defense Technology, Changsha 410073, China
2 Institute of Space and Earth Information Science, The Chinese University of Hong Kong, Hong Kong 999077, China

Abstract In electronic speckle pattern interferometry (ESPI), because saw-tooth phase map obtained by phase-shifting is inherently full of speckle noise, noise reduction should be carried out to suppress high-level noise before it is unwrapped. In accordance with the feature of the saw-tooth phase map, an adaptive filter method combining the classical sine/cosine filter and the fringe orientation information of the phase map is developed. A fringe orientation map is first generated from the saw-tooth phase map, and then a fringe-contoured window is derived accordingly. Finally, filtering is carried out within the window. Compared with existing filters, it has a better performance on phase jump information preservation without any blurring effect on phase distribution provided that filtering is implemented on the equal-phase window. Moreover, its capability for noise reduction is more powerful. The effectiveness and advantages of the novel filter have been also verified by both simulated and real saw-tooth phase maps.

Keywords optical measurement, electronic speckle pattern interferometry (ESPI), phase-shifting, saw-tooth phase map, filtering

1 Introduction

Phase-shifting, one of the most important achievements in electronic speckle pattern interferometry (ESPI), has high applicability and remains the primary choice in processing fringe patterns today as long as conditions permit [1,2]. However, since the phase image obtained by phase-shifting is a saw-tooth phase map with an arrangement of $(-\pi, +\pi]$, unwrapping should be carried out to generate a continuous phase image. Although the principle is easy to follow, the actual ESPI saw-tooth phase map contains a large amount of noises, which poses great difficulties for unwrapping. Therefore, denoising becomes a necessity prior to unwrapping.

Neither an average filter nor median filter can be adopted directly to denoise the saw-tooth phase map because they seriously damage its jump information. Capanni et al. [3] proposed an improved median filter, which can be summarized as follows: 1) calculate the histogram according to the grey information in the filter window; 2) calculate the positional relation of the filter window and the phase jump line based on the result of 1); 3) obtain final filtered results according to all or part of the information in the filter window. Capanni's method maintains the phase jump information comparatively well, although miscalculation is still inevitable. Huang et al. [4] made an improvement of Capanni's method by further partitioning the histogram. Qian et al. [5] adapted Capanni's method to make the window size variable. Aebischer et al. [6] put forward a sine/cosine filtering method as follows: 1) decompose the saw-tooth map into two images through sine and cosine calculation; 2) denoise both images respectively through an average filter; 3) obtain the results by calculating inverse tangent. Experiments show that the sine/cosine filter is easy to use and effective in eliminating the inconsistent points while maintaining the jump information of the phase. Palacios et al. [7] proposed a method combining sine/cosine filter and mask filter.

Fringe orientation contains significant information necessary for automatic processing of fringe patterns [8], which provides foundations for speckle pattern denoising [9], phase extraction [10], etc. In this article, fringe orientation information is applied to an ESPI saw-tooth phase map, and a fringe-contoured-window sine/cosine filter (FCW-SCF) which suits the characteristics of the phase map is further proposed. Compared with existing filters, FCW-SCF has the following advantages: 1) good maintenance of the jump information of the saw-tooth phase map; 2) zero damage to phase information as the filtering is conducted on the contoured phase map; 3) clearer elimination of the speckle noise in the saw-tooth phase map.

Translated from *Acta Optica Sinica*, 2007, 27(5): 864–870 [译自: 光学学报]

E-mail: fusihua2002cn@hotmail.com

2. Principles of FCW-SCF

2.1 Fringe orientation obtained by gradient method

Among existing methods of calculating fringe orientation, gradient method [8] is relatively easy to apply and thus in frequent use. The definition and calculation of the ESPI interferometric fringe pattern will be given first before the calculation of the orientation of the ESPI saw-tooth phase map is introduced.

The orientation of the saw-tooth phase map is defined as

$$\theta(x,y) = \arctan\left[\frac{\partial\phi(x,y)}{\partial y} \Big/ \frac{\partial\phi(x,y)}{\partial x}\right] \pm \frac{\pi}{2}, \tag{1}$$

where $\theta(x, y)$ is the fringe orientation to be calculated, and $\phi(x,y)$ is the fringe phase. Equation (1) can be applied directly if there were no noises. However, noises are comparatively high in actual interferometric fringe patterns and it becomes a primary necessity to smooth the fringe patterns. In actual calculation, Eq. (2) is generally adopted to obtain fringe orientation:

$$\theta(x,y) = \frac{1}{2}\arctan\frac{\sum\limits_{(m,n)\in S} 2G_x(m,n)G_y(m,n)}{\sum\limits_{(m,n)\in S}\left(G_x^2(m,n) - G_y^2(m,n)\right)} \pm \frac{\pi}{2}, \tag{2}$$

where $G_x(m,n)$ and $G_y(m,n)$ are gradients on the x and y direction, respectively, and S is the size of the window adopted to estimate fringe orientation.

The saw-tooth phase map has an obvious 2π jump in its phase distribution, which prevents the use of Eq. (2) directly to compute the fringe direction. However, its resultant sine and cosine map both have continuous phase, which provides the possibility to extend the orientation estimation method. First, the saw-tooth phase map is converted into the sine and cosine map through a simple sine and cosine operation referring to the principle of sine/cosine filter. A continuous sine and cosine map whose orientation remains the same as that of the original saw-tooth phase map (illustrated clearly by Eq. (3)) can thus be obtained. The orientation of the saw-tooth map can be obtained by computing the orientation of the corresponding sine or cosine map through the gradient method:

$$\begin{cases} \dfrac{\partial \sin\phi}{\partial y} \Big/ \dfrac{\partial \sin\phi}{\partial x} = \dfrac{\cos\phi \dfrac{\partial\phi}{\partial y}}{\cos\phi \dfrac{\partial\phi}{\partial x}} = \dfrac{\dfrac{\partial\phi}{\partial y}}{\dfrac{\partial\phi}{\partial x}}, \\ \dfrac{\partial \cos\phi}{\partial y} \Big/ \dfrac{\partial \cos\phi}{\partial x} = \dfrac{-\sin\phi \dfrac{\partial\phi}{\partial y}}{-\sin\phi \dfrac{\partial\phi}{\partial x}} = \dfrac{\dfrac{\partial\phi}{\partial y}}{\dfrac{\partial\phi}{\partial x}}. \end{cases} \tag{3}$$

The orientation estimation procedure of the saw-tooth phase map is summarized as follows:

Step 1 Transform the saw-tooth phase map into a sine or cosine map (both can be used to calculate the fringe orientation; here the sine map is discussed in illustration).

Step 2 Smooth the sine map to reduce noises. Average filtering is then conducted multiple times with small windows (3×3 or 5×5) until satisfactory results are obtained. Reference [8] proposes a smoothing on the fringe pattern by Gaussian filter and provides a detailed analysis on the influences of each parameter.

Step 3 Calculate the gradient vector field of the smoothed sine map using Sobel, Prewitt, Roberts or other gradient operators. The Marr-Hildreth operator is an alternative, especially when considering its good denoising performance, although the complexity of calculation is increased consequently.

Step 4 Use Eq. (2) to calculate the fringe orientation on every point of the gradient vector field. The size of the window (S, and r is radius) is an important parameter, which should vary in accordance with the density of the fringe because it exerts great influence over the accuracy of orientation estimation. We have done repeated fringe estimation experiments on a great amount of simulated fringe patterns and reached the following conclusions: S used in orientation estimation should be set 1 to 1.2 times the width of the widest fringe of the fringe pattern as a general rule; larger windows can improve the accuracy but are not noticeable, and calculation work is increased radically.

Fringe orientation acquired in this way ranges from 0 to π. Figure 1 is an actual ESPI saw-tooth phase map with a fringe width of about 45 pixels obtained by phase-shifting method. Figure 2 shows its orientation image calculated by gradient method, where r is 21 (the image grey level 0 represents orientation 0 and the grey level 255 orientation π).

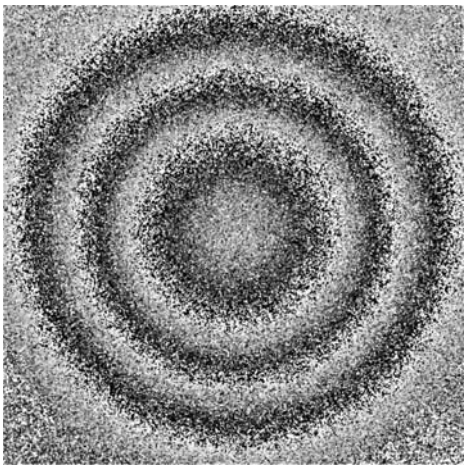

Fig. 1 Real saw-tooth phase map derived by phase-shifting method

Fig. 2 Fringe orientation map of Fig. 1 derived by gradient method

2.2 Determination of fringe-contoured window

The interferometric fringe's obvious fringe orientation flow can be tracked along the fringe tangential direction to obtain the fringe contour. Suppose the coordinate of the current pixel is $P_0(x_0, y_0)$ with its fringe orientation of θ_0. We track it along the positive and negative directions of the fringe respectively and obtain two pixels $P_1(x_1, y_1)$ and $P_{-1}(x_{-1}, y_{-1})$ adjacent to the current pixel:

$$\begin{cases} x_1 = x_0 + \cos\theta_0, \\ y_1 = y_0 + \sin\theta_0, \end{cases}$$

$$\begin{cases} x_{-1} = x_0 - \cos\theta_0, \\ y_{-1} = y_0 - \sin\theta_0. \end{cases}$$

Continue following to obtain $P_n(x_n, y_n)$ and $P_{-n}(x_{-n}, y_{-n})$ yields general equations of tracking (shown in Fig. 3(a)):

$$\begin{cases} x_{n+1} = x_n + \cos\theta_n, \\ y_{n+1} = y_n + \sin\theta_n, \end{cases}$$

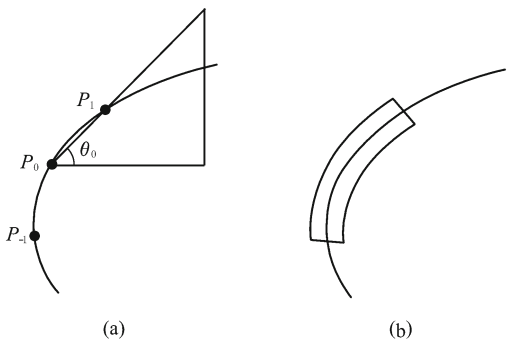

Fig. 3 (a) Fringe contour derived by tracking along fringe direction; (b) fringe-contoured window derived by expanding fringe contour in normal direction

$$\begin{cases} x_{-n-1} = x_{-n} - \cos\theta_{-n}, \\ y_{-n-1} = y_{-n} - \sin\theta_{-n}. \end{cases}$$

Finally, a curve covering point (x_0, y_0) along the direction of the fringe – the fringe contour line – is obtained as shown in Fig. 3(a). A fringe-contoured window will be formed if this curve is extended to both sides, as shown in Fig. 4.

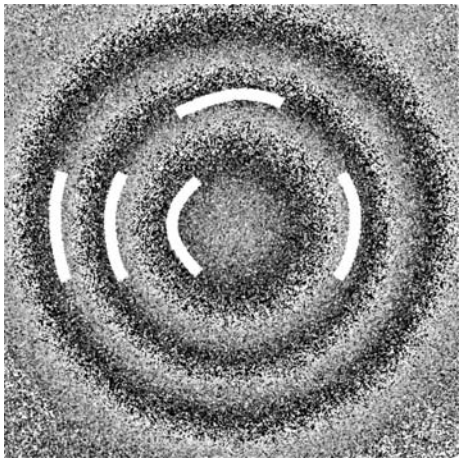

Fig. 4 Scheme of fringe-contoured window of Fig. 1

A digital image determines its values on integer pixels only, whereas the point (x_n, y_n) acquired by the aforementioned method is not necessarily an integer point. To deduce the discrete error, the bilinear interpolations of the fringe orientations of the four points adjacent to the non-integer point can be adopted as the fringe orientation of (x_n, y_n). In addition, an accumulation error takes place because of the point-wise tracking used in the approach. Since the error is related with both fringe pattern error and the accumulation step number, it can be controlled within a certain range if the proper accumulation number is taken.

2.3 Filtering within fringe-contoured window

Once the fringe-contoured window of the saw-tooth phase map is determined, sine/cosine filtering can be carried out. The following model [11] can describe the phase and noise of the map:

$$\hat{\phi} = \phi + n,$$

where $\hat{\phi}$ is measuring phase containing noises, ϕ the theoretical noise-free phase, and n the Gaussian distribution noise.

To solve the problem of 2π jump in filtering the saw-tooth phase map, we first decompose it into a sine and cosine map and then low-pass filter them respectively in a fringe-contoured window. Finally, a filtered saw-tooth

phase map will be generated by inverse tangent transforming the filtered sine and cosine maps. Suppose $\tilde{\phi}$ is the intended phase after filtering $\hat{\phi}$, the aforementioned filtering process can be described as

$$\tilde{\phi} = \arctan\frac{\sum \sin(\phi+n)}{\sum \cos(\phi+n)} = \arctan\frac{\sum \sin\phi\cos n + \sum \cos\phi \sin n}{\sum \cos\phi\cos n - \sum \sin\phi \sin n}. \quad (4)$$

Because filtering is conducted only in the fringe-contoured window, the phase ϕ remains, i.e., $\sin\phi$ and $\cos\phi$ are fixed values. In this case, Eq. (4) can be represented as

$$\tilde{\phi} = \arctan\frac{\sin\phi\sum\cos n + \cos\phi\sum\sin n}{\cos\phi\sum\cos n - \sin\phi\sum\sin n}. \quad (5)$$

The following expressions exist provided S is sufficiently large:

$$\sum \sin n = 0, \quad \sum \cos n > 0.$$

Thus it can be deduced from Eq. (5):

$$\tilde{\phi} = \arctan\frac{\sin\phi\sum\cos n}{\cos\phi\sum\cos n} = \arctan\frac{\sin\phi}{\cos\phi} = \phi. \quad (6)$$

Equation (6) proves it possible to thoroughly filter speckle noise in a fringe-contoured window without blurring or distorting the saw-tooth phase map.

Typically, since one FCW-SCF filtering fails to achieve satisfactory results due to the high noise level of the ESPI saw-tooth phase map, multiple filtering is recommended according to the noise level.

3 Experimental results and analysis

To test the efficiency of FCW-SCF, we conducted filtering on a simulated saw-tooth phase map and real saw-tooth phase map.

3.1 Filtering simulated saw-tooth phase map

Figure 5(a) shows a simulated saw-tooth phase map added with Gaussian noise of standard variance 60. The width of the fringe in the center is approximately 7 pixels, and the width of the margin fringe is approximately 12 pixels.

Figure 5(b) shows the result obtained after three times' 3×3 sine/cosine filtering on Fig. 1. It is observed that noise is relatively suppressed while inconsistent points scatter in the middle as well as on the margin of the map. Figure 5(c) is the result after 3×3 sine/cosine filtering nine times; the inconsistent points on the margin are reduced but phase distortion is seen in the middle. Figure 5(d) shows the result after 5×5 sine/cosine filtering thrice; here the inconsistent points on the margin are further reduced, but the phase blurring is more serious. Figure 5(e) is the result after 5×5 sine/cosine filtering six times. In summary, the traditional sine/cosine filter is ineffective in producing satisfactory results whether the filer window is enlarged or filtering is increased several times. In contrast, Fig. 5(f), which is obtained by 3×9 FCW-SCF filtering on Fig. 5(a) thrice, presents an excellent result on both the center and margin of the saw-tooth phase map now devoid of any speckle noise. Moreover, the phase information receives no damage at all because the filtering is operated in a fringe-contoured window.

3.2 FCW-SCF on simulated saw-tooth phase map

Figure 6(a) is a simulated saw-tooth phase map added with Gaussian noise of variance 60. Figure 6(b) shows the result obtained by 3×3 sine/cosine filtering six times; inconsistent points fill the map which makes the phase unwrapping impossible. Again both an increase in filtering number and enlargement of the filter window only lead to further blurring of the phase. Figure 6(c) shows the result after 3×15 FCW-SCF filtering thrice; phase inconsistent points are eliminated totally without any damage on phase distribution. Any unwrapping method can be adopted on Fig. 6(c) to achieve expected results.

3.3 Filtering a real saw-tooth phase map

Figure 7(a) is a real saw-tooth phase map with variable-density full of shearing speckle noises. Figure 7(b) shows the clear removal of the noises after 3×15 FCW-SCF filtering thrice. Figure 7(c) is the continuous phase map after unwrapping. Figures 8(a), 8(b), and 8(c) are the phase distributions of Figs. 7(a), 7(b), and 7(c) on the same cross-section. On cross section A-A′, noise is so grave that the phase jump points become indistinguishable from the phase inconsistent points. On cross section B-B′, phase inconsistent points are erased completely and phase jump information remains undamaged. On cross section C-C′, the phase is restored fully by simple unwrapping.

Both simulated and real experiments prove that the proposed FCW-SCF works better than the previous sine/cosine filter in noise elimination, especially on the saw-tooth phase map with variable fringe density. The sine/cosine filter is usually unable to deduce noise all over the map. Its efficiency could be improved on the low-fringe-density area when the filter window is enlarged or filtering is repeated, but at the price of blurring on the high-fringe-density area and damage to phase jump information. The FCW-SCF is a good solution to the problem as it offers ideal deduction of noises over the entire map and keeps the jump information intact. This advantage becomes even more prominent especially when noise level is high.

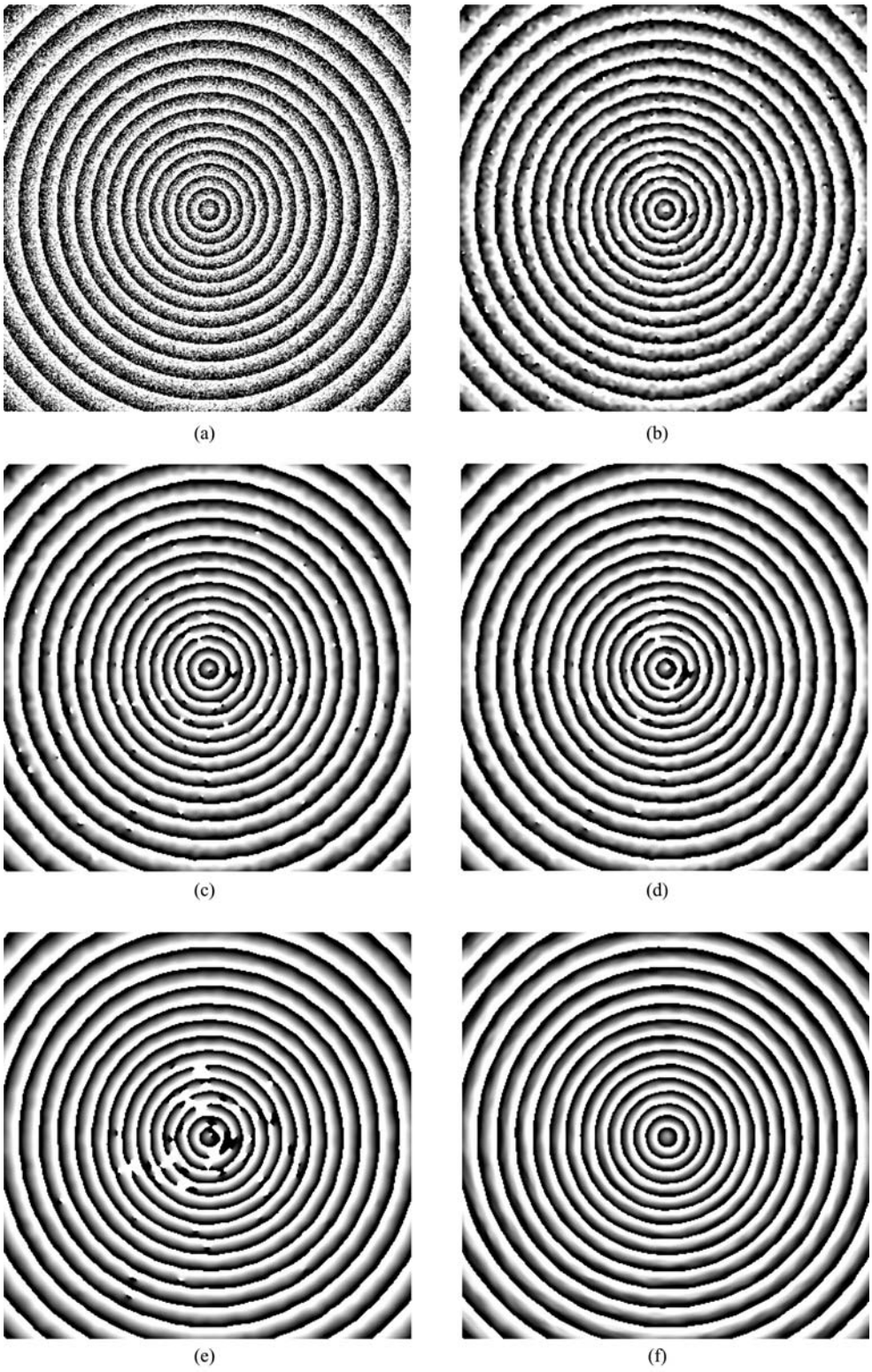

Fig. 5 (a) Simulated saw-tooth phase map; (b) resultant map filtered three times by sine/cosine filter with a window size of 3 × 3; (c) resultant map filtered nine times by sine/cosine filter with a window size of 3 × 3; (d) resultant map filtered three times by sine/cosine filter with a window size of 5 × 5; (e) resultant map filtered six times by sine/cosine filter with a window size of 5 × 5; (f) resultant map filtered three times by FCW-SCF with a window size of 3 × 9

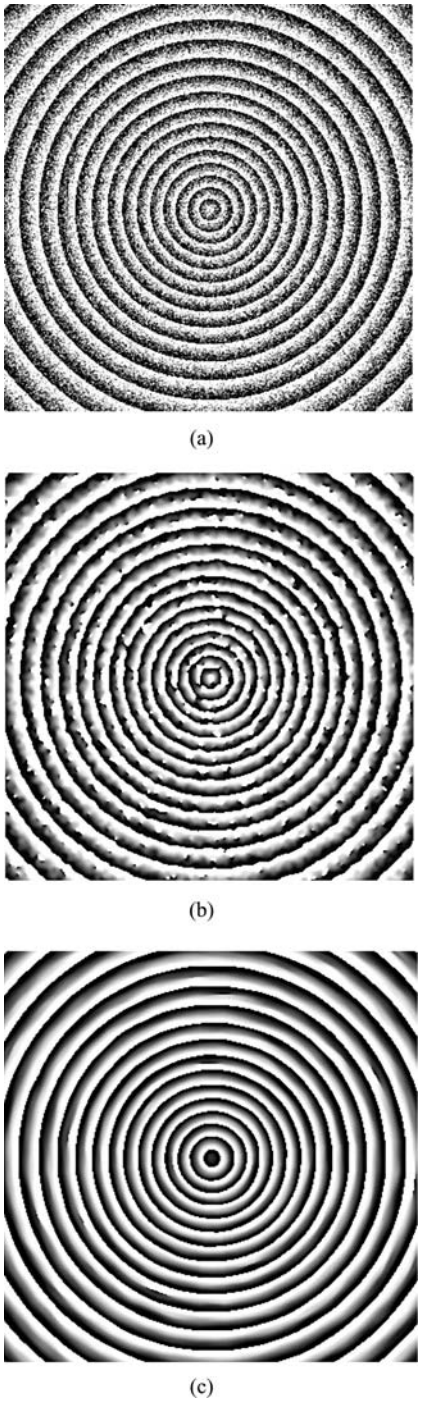

Fig. 6 (a) Simulated saw-tooth phase map; (b) resultant map filtered six times by sine/cosine filter with a window size of 3×3; (c) resultant map filtered three times by FCW-SCF with a window size of 3×15

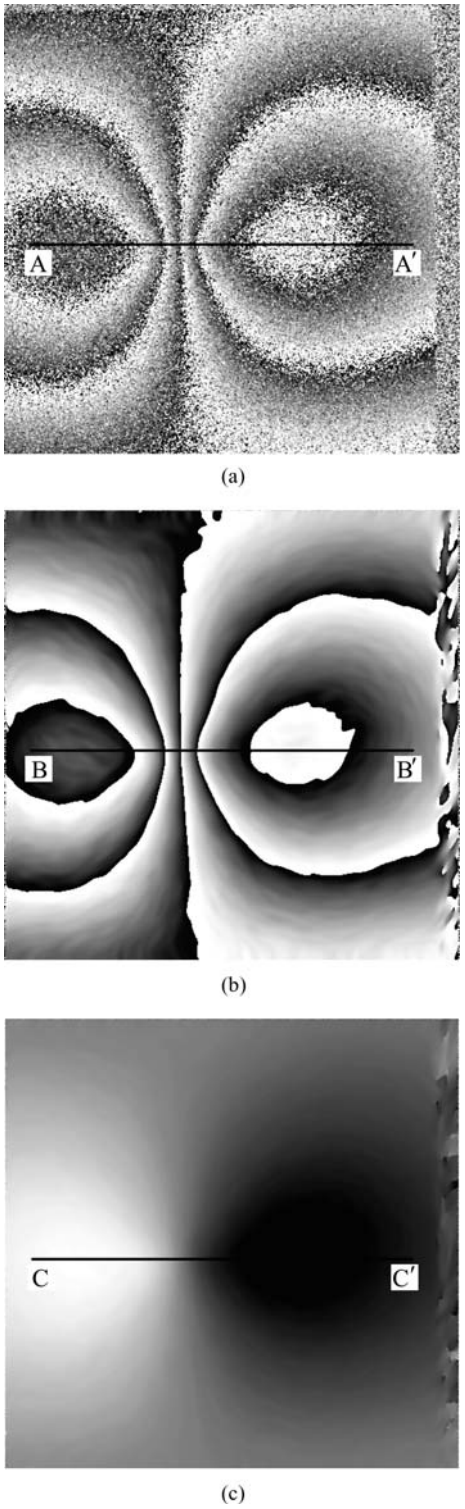

Fig. 7 (a) Real saw-tooth phase map; (b) resultant map filtered three times by FCW-SCF with a window size of 3×15; (c) unwrapped phase map

4 Conclusions

Phase-shifting, one of the major data processing methods, only generates a saw-tooth phase map which requires further unwrapping to transform into a continuous phase map. An actual ESPI saw-tooth phase map contains a large quantity of noises that require denoising before unwrapping in general. This article proposes a contoured sine/cosine filter which makes full use of fringe orientation information. Compared with existing methods, it has the following merits: 1) good maintenance of the jump information in the saw-tooth phase map; 2) zero damage on phase information because filtering is

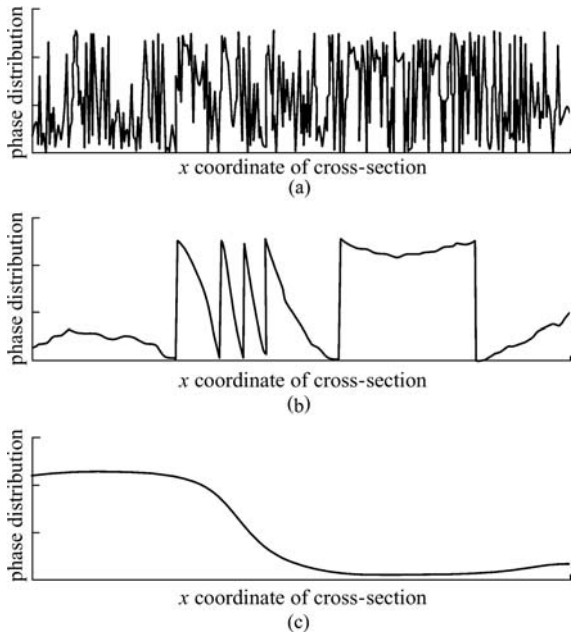

Fig. 8 Phase distributions of three cross-sections. (a) A-A′ in Fig. 7(a); (b) B-B′ in Fig. 7(b); (c) C-C′ in Fig. 7(c)

conducted on the contoured phase line; 3) better speckle noise deduction in the saw-tooth phase map. The effectiveness of the method is evident in experiments on both simulated and real maps: the saw-tooth phase map filtered by FCW-SCF is almost entirely free of any speckle noise and a simple unwrapping method can suffice in phase restoration.

Acknowledgements This work was partly supported by the National High Technology Research and Development Programs of China (Grant No. 2007AA12Z121).

References

1. Creath K. Phase-shifting speckle interferometry. Applied Optics, 1985, 24(18): 3053–3058
2. Kwon O Y, Shough D M, Williams R A. Stroboscopic phase-shifting interferometry. Optics Letters, 1987, 12(11): 855–857
3. Capanni A, Pezzati L, Bertani D, et al. Phase-shifting speckle interferometry: a noise reduction filter for phase unwrapping. Optical Engineering, 1997, 36(9): 2466–2472
4. Huang M J, Sheu W H. Histogram-data-orientated filter for inconsistency removal of interferometric phase maps. Optical Engineering, 2005, 44(4): 045602
5. Qian F, Wang X, Wang X, et al. Adaptive filter for unwrapping noisy phase image in phase-stepping interferometry. Optics and Laser Technology, 2001, 33(7): 479–486
6. Aebischer H A, Waldner S. A simple and effective method for filtering speckle-interferometric phase fringe patterns. Optics Communications, 1999, 162(4–6): 205–210
7. Palacios F, Goncalves E, Ricardo J, et al. Adaptive filter to improve the performance of phase-unwrapping in digital holography. Optics Communications, 2004, 238(4–6): 245–251
8. Zhou X, Baird J P, Arnold J F. Fringe-orientation estimation by use of a Gaussian gradient filter and neighboring-direction averaging. Applied Optics, 1999, 38(5): 795–804
9. Yu Q F, Sun X Y, Liu X L, et al. Spin filtering with curve windows for interferometric fringe patterns. Applied Optics, 2002, 41(14): 2650–2654
10. Marroquin J L, Rodriguez-Vera R, Servin M. Local phase from local orientation by solution of a sequence of linear systems. Journal of the Optical Society of America A, 1998, 15(6): 1536–1544
11. Nico G. Noise-residue filtering of interferometric phase images. Journal of the Optical Society of America A, 2000, 17(11): 1962–1974